# HIGH IMPULSE NOISE INTENSITY REMOVAL IN MRI IMAGES

*M. Mafi, H. Martin, M. Adjouadi*

Center for Advanced Technology and Education, Florida International University, Miami, Florida, USA
{mmafi002, hmart027, adjouadi}@fiu.edu

***Abstract*— This study introduces an image denoising method which focuses on detail preservation in the presence of high impulse (salt and pepper) noise. The proposed adaptive median and fixed weighted mean filter (AMFWMF) result in enhanced image similarity and optimal edge information preservation with high correlation and structural similarity index measures. For comparative purposes, a comprehensive analysis of other denoising filters is provided based on different structural metrics. Such standard measures, are used as standard measurements to gauge which of these methods leads to an optimal outcome. The provided results are compared to other existing denoising filters and support of hypothesis of a filter with high resilience to impulse noise of high density levels, our assertion on the method's resilience to impulse noise even under high-density levels. Then, we apply it to a set of MRI images corrupted by different levels of impulse noise intensity.**

## I. INTRODUCTION

Noise remains a ubiquitous and unwanted phenomenon that is inherent to many image acquisition and transmission process. One such type of noise that degrades image quality is impulse (salt and pepper) noise which appears as white and black pixels in the degraded image. In order to remove this type of noise, smoothing filters are often applied, while attempting to preserve important details present in the image.

In this study, we assume the noise model as given by (1), assuming normalization:

$$I_c = \begin{cases} 0 & Probability\ P_p \\ 1 & Probability\ P_s \\ C & Probability\ 1 - P_p - P_s \end{cases} \quad (1)$$

In [1], $C$ denotes the uncorrupted pixels, corrupted pixels are assigned probabilities $P_s$ (salt) and $P_p$ (pepper).

This kind of noise imposes a challenge to de-noise images specially, MRI`s, often resulting in missing details or, conversely, in false edges. Therefore, this study introduces a new filter which combines the strengths of the median filter and those of fixed mean filter to preserve image details, true edges, and overcoming the presence of impulse noise even under high density levels. The results obtained are contrasted to other well-known denoising filters by using different structural metrics and evaluation measures to gauge the degree of edge preserving by means of correlation and structural similarity index (SSIM). The mean filter, although effectively in attenuating the presence of high impulse noise, tends to introduce more blur in the image, which in turn could lead to further loss of details. To prevent these unwanted side effects, we keep the size of the mean filter small and fixed. The block-wise adaptive filter [2] introduces a method in order to reduce impulse noise in MRI images, it is based on a traditional adaptive median filter (AMF) and detects the impulse noise and adaptively adjust the size of the filter. However, it does not have good performance in the presence of high intensity impulse noise. The comprehensive survey on switching median filters in [3] provides a comparative assessment of predominant denoising filters such as the standard median filter [4], center weighted median (CWMF) [5], the weighted median filter [6], the adaptive switching median (ASMF) [7] and the modified decision based unsymmetrical trimmed median (MDBUTMF) [8]. The results indicate that MDBUTMF [8] is the best of them [3].

This paper also provides a comparative assessment contrasting the results obtained using the proposed method with the results of the most recent and proven filters, including the improved boundary discriminative noise detection filter (IBDND) [9] an improvement on BDND [10], unsymmetrical trimmed modified winsorized mean filter (DBUTMWMF) [11], Unbiased weighted mean Filter (UWMF) [12], and the Lu`s three-values-weighted filter [13]. The results presented in [12] were better than those obtained using adaptive median filter (AMF) [14], MDBUTMF [8], IBDND [9], cloud model filter (CMF) [15] as well as the Interpolation Based and Impulse Noise Filter (IBINRF) [16].

## II. PRPOSED METHOD

With the proposed method, boundary edges of filtered image are assumed to have high correlation with the original image; as such, edges should track the true routes even under high density impulse noise. Most of the current leading filters ensure good impulse noise reduction figures, but they still do not perform well on boundaries, especially in the presence of high density impulse noise. They also perform purely on MRI images, especially in presence of high intensity impulse noise.

When using an adaptive median filter, all pixels with 0 and 1 values are removed from the initial sliding window. The median value of the remaining pixels, within the window with probability of $1 - P_p - P_s$ as in (1), is used as the filtered value for the pixel being processed. If all of them are 0s, 1s or a combination of them, then the size of the window is increased by 1 and the process is repeated until the window size reaches the predefined maximum window size.

By increasing the size of the adaptive median filter window, the structural metrics will be somewhat decreased, due to a slightly blurred image. However, the edges still be sharp. Therefore, it appears that there is a tradeoff to be made between the edges extracted and the quantitative values of the structural metrics. However, the pixel being processed will remain unchanged if the maximum window size is reached and it only contains 0s and 1s, or a combination of them. There are special cases when a given texture will consists of 1s and 0s. These textures are especially challenging to delineate in the presence of high intensity impulse noise. When such combinations of 0s and 1s are found in several instances in the sliding window, the mean filter needs to be applied. This combination can smooth the image while maintaining high structural metrics and sharp edge boundaries. In order to avoid any lingering noise in the black and white regions (especially in relatively bigger ones) in which the mean filter changes the intensities, an additional shrinkage window can be defined before applying the mean filter. This step, which removes 0s in white regions and 1s in black regions, can be very useful for textures that consist of combinations of black and white. Hence, the maximum window size of the window would depend on the texture and noise level in the image being denoised.

The structural metrics for the fixed mean filter can be improved by assigning appropriate adaptive weights for the pixels in the selected window in accordance to (2). This window could contain all 0s ($P_p$), all 1s ($P_s$), or a combination of them together with the other pixels with probability of $1 - P_p - P_s$, as indicated earlier in (1).

$$\omega_{x,y} = m * d\ ,\ d = (|x - i|^p + |y - j|^p)^{1/p} \qquad (2)$$

In (2), $d$ is the Minkowski distance [13] of the selected window, and $m$ is a variable which depends on the texture (the next section explains how this variable is selected). In this equation, if $p = 1$, then the best structural metrics is obtained, which is the case of this study. The mean filter tends to introduce more blur in the image, which in turn could lead to loss of detail. To prevent theses side effects, the size of the mean filter should be kept small and fixed, as in the proposed method. Figure 1 shows a flow chart depicting the process, its steps are discussed in details in the next sub-section.

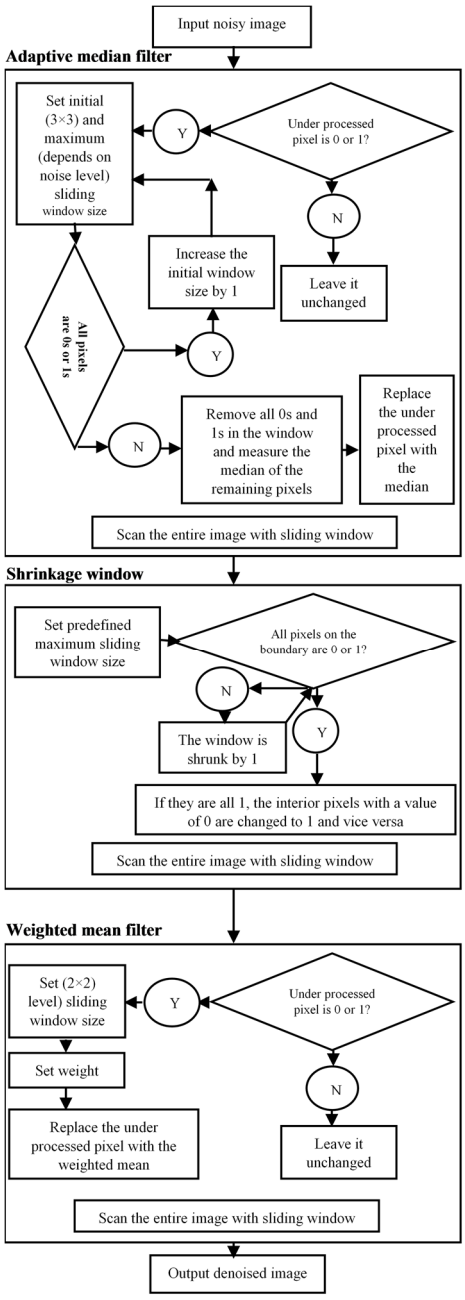


Figure 1. Process flow chart

### *A. Structure of the Method*

Implementation of the method assumes the following steps:

1. When deploying the adaptive median filter, if all of the pixels in the 3×3 window are 0s or 1s, then, the size of the window is increased to a 4×4, and

if the same conditions persist the size of the kernel is further increased until the maximum kernel size is reached or the conditions are no longer met. We then arrange the normalized pixels of the 2-D selected window as $1 \times N$ 1-D vector and check if the pixel $I(i,j)$ being processed, at the center of the kernel window, is a corrupted pixel; that is, we check if $I(i,j) = 0$ or 1 (normalized value) in $W_{1\times N}(\dots, I(i,j), \dots)$. If the pixel is not corrupted, proceed to 4.

2. Detect all pixels with 0 and 1 values, and eliminate them, so the size of the window $W_{1\times N}$ is now decreased to a new size $W_{1\times N-k} = (\dots, I(i,j), \dots)$, where $k$ represents the number of corrupted pixels that were removed.
3. Replace the $I(i,j)$ pixel value with the median value of the remaining $N-k$ pixels in the vector window if at least one pixel remains in the reduced window, otherwise leave $I(i,j)$ unchanged
4. Slide the window by one pixel and return to step 1 and repeat until the entire image has been processed resulting in an adaptive median filtered image.
5. Starting from the predefined maximum size for the shrinkage window, we start by checking the boundary pixels of the selected window. One of the following condition has to be met: If they are all 1, the interior pixels with a value of 0 are changed to 1. If all the pixels on the boundary are 0, then the interior pixels with a value of 1 are changed to 0. Otherwise, the window is then shrunk by one and the process is repeated until the minimum size (3×3) is reached.
6. For the fixed mean filtered image, use a 2×2 window in a convolution manner, and check if the pixel being processed ($I(i,j)$ within the vector window $W_{1\times 4} = (I(i,j), I(i,j+1), I(i+1,j), I(i+1,j+1))$ is corrupted (i.e., $I(i,j) =$0 or 1 (normalized value))
7. Using the weights defined in (2), if salt or pepper (probability $P_s$ or $P_p$) is detected, the new processed pixel would be assigned the new value as in (3). Otherwise, it leaves the pixels unchanged.

$$I_{new}(i,j) = \frac{\sum_{(x,y)\in W_{new(i,j)}} \omega_{x,y}\, I_{x,y}}{N-1} \qquad (3)$$

In these equations, $N$ is 4, $W_{new(i,j)} = \{\mathrm{I(i,j+1)}, \mathrm{I(i+1,j)}, \mathrm{I(i+1,j+1)}\}$, indices $(i,j)$ point to the position of the corrupted pixel, and $(x,y)$ are the coordinates of the pixels around it. In this proposed method, when the detected corrupted pixel occurs as salt or pepper (with probabilities $P_s$ or $P_p$), the variable $m$ is selected according to one of these conditions:

- If $sum \geq N-1$; $for\ sum = 2I(i,j+1) + 2I(i+1,j) + I(i+1,j+1)$, where $I(i,j+1)$ is the east pixel, $I(i+1,j)$ is the south pixel, and $I(i+1,j+1)$ is the southeast pixel. Then, set $m = 1$ for the east and south pixels and $m =$ 0.5 for the southeast pixel.
- If $sum < N-1$; $for\ sum = 2I(i,j+1) + 2I(i+1,j) + I(i+1,j+1)$ , where $I(i,j+1)$ is the east pixel, $I(i+1,j)$ is the south pixel, and $I(i+1,j+1)$ is the southeast pixel. Then, set $m = 2$ for the east and south pixels and $m =$ 0.5 for the southeast pixel. However, if the neighboring pixels are equal, then, set $m = 1$ for the east and south pixels and $m = 0.5$ for the southeast pixel.

8. Leave uncorrupted pixels unchanged.
9. Repeat steps 6-8 for the entire filtered image. Check the level of impulse noise present, and if the filter component yields satisfactory results. If results are not satisfactory, increase the adaptive median filter window size by two and repeat until optimal results are obtained. Table 1 shows the maximum size of adaptive median filter in order to get satisfactory results for different noise levels.

| *Window size* | *3×3* | *5×5* | *7×7* | *9×9* | *> 9×9* |
|---|---|---|---|---|---|
| *Noise level* | < 40% | ≥ 40% ≤ 70% | > 70% ≤ 80% | > 80% ≤ 90% | > 90 |

*Table 1. Maximum window size of adaptive median filter with different noise levels on Lena, Camera man, MRI images*

### *B. Evaluation Measures*

To measure the degree of edge preserving and image structural metrics, Correlation Coefficient ($\beta$) and Peak Signal to Noise Ratio (PSNR) are computed. The correlation coefficient is defined as follows

$$\beta = \frac{\sum_{i=0}^{M-1}\sum_{j=0}^{N-1}[x(i,j)-\overline{x(i,j)}]\times[y(i,j)-\overline{y(i,j)}]}{\sqrt{\sum_{i=0}^{M-1}\sum_{j=0}^{N-1}[x(i,j)-\overline{x(i,j)}]^2 \times [y(i,j)-\overline{y(i,j)}]^2}} \qquad (4)$$

Where $M$ and $N$ are image sizes, $x(i,j)$ represent the pixels in the original noise-free image, $y(i,j)$ represent the pixels in the denoised image after the filtering process has been applied, $\overline{x(i,j)}$ and $\overline{y(i,j)}$ represent the mean values of the $x$ and $y$ images, respectively.

The structural similarity index (SSIM) [17] is computed as follows:

$$\mathrm{SSIM} = \frac{(2\bar{x}\bar{y}+C1)(2\sigma_{xy}+C2)}{(\bar{x}^2+\bar{y}^2+C1)({\sigma_x}^2+{\sigma_y}^2+C2)} \qquad (5)$$

Where $\sigma_x$ and $\sigma_y$ are the standard deviations for the $x$ and $y$ images respectively, and $\sigma_{xy}$ is the standard deviation of the two images combined.

$C_1$ and $C_2$ are variables that depend on the dynamic range of pixels, often set to $C_1 = 0.01L$ and $C_2 = 0.03\,L$. $L$ is the dynamic range (we set it to 1 for our experiment since images are normalized). The default values for $C$ are recommended by the inventors of the SSIM measure to stabilize the denominator and divisions by zero.

Figures 2 and 3 show, the edge boundaries and similarity of different natural and MRI images after applying the proposed filter in the presence of high intensity noise.

## III. RESULTS AND DISCUSSION

To assess the merits of the proposed method, different natural and MRI input images are used for evaluation. For comparative purposes, the results obtained using the proposed method are compared with some of the most effective methods reported in the literature, namely IBDNDF [9], DBUTMWMF[11], UWMF [12] and Lu`s three-values-weighted filter [13], on the different images and under different impulse noise intensities. All the parameters chosen for comparing filters, such as initialization and regularization parameters, weights, and window sizes, are set according to their proposed optimal values for the specific noise level.

Tables 2 and 3 show the results obtained on the correlation ($\beta$), and the structural similarity index (SSIM) measures, comparing different filters against the proposed filter (results for the proposed filter are based on the minimum and maximum initial window size of the adaptive median filter for the related noise level). All these metrics are computed in the presence of 10 to 90 percent impulse noise on images frequently used in the literature for the denoising purposes (i.e. “Lena” and “Cameraman”) and MRIs.

Figures 4 and 5 show the same comparison in the presence of 80% and 90% impulse noise, respectively, on MRI images. Figure 6 show the results obtained from the proposed method for 20%, 40%, 60%, 80% and 90% impulse noise on different MRI images.

As these figures show, the proposed algorithm has good performance in terms of keeping relevant detail and obtaining the highest similarity, least noise, and preserving edges, especially in high impulse noise environments.

## IV. SUMMARY

In this study, a new combination of median and mean filter, we refer to as the adaptive median and fixed weighted mean filter (AMFWM), was introduced as a new smoothing filter to optimally remove or minimize the presence of impulse noise even when high density levels are present. This combination of filters is shown

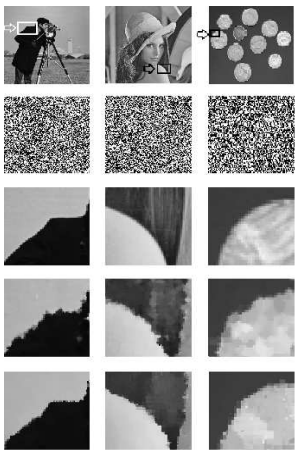

Figure 2. Edges on the specified areas indicated within the boxes shown for: “Camera man” with 90% intensity impulse noise, “Lena” with 90% impulse noise, and “Coins” with 90% impulse noise in columns 1 through 3, respectively. After applying the filter: Rows 1 through 5 are: Original image showing the specified area under scrutiny, noisy image, original specified area, and the denoised results using, UWMF and AMFWMF filters.

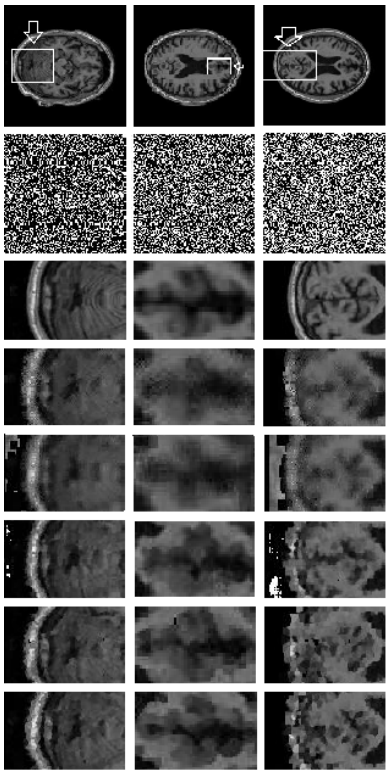

Figure 3. Results of filtering MRI images with 70%, 80% and 90% impulse noise intensity in column 1 through 3, respectively. After applying the filter: Rows 1 through 8 are: Original image showing the specified area under scrutiny, noisy image, original specified area, denoised results using, IBDNDF [9], DBUWMF [11] UWMF [12] and Lu`s three-values-weighted filter [13], and AMFWMF filters.

| | *IBDNDF [9]* | | | *DBUTMWMF [11]* | | | *UWMF [12]* | | | *Lu`s three-values-weighted [13]* | | | ***AMFWMF*** | | |
|---|---|---|---|---|---|---|---|---|---|---|---|---|---|---|---|
| | *Lena* | *Camera man* | *MRI image* | *Lena* | *Camera man* | *MRI image* | *Lena* | *Camera man* | *MRI image* | *Lena* | *Camera man* | *MRI image* | ***Lena*** | ***Camera man*** | *MRI image* |
| *10%* | 0.9720 | 0.9567 | 0.9971 | 0.9722 | 0.9581 | 0.9434 | 0.9725 | 0.9586 | 0.9983 | 0.9714 | 0.9576 | 0.9975 | **0.9843** | **0.9821** | **0.9987** |
| *20%* | 0.9704 | 0.9518 | 0.9929 | 0.9712 | 0.9543 | 0.8621 | 0.9717 | 0.9566 | 0.9909 | 0.9687 | 0.9525 | 0.9936 | **0.9834** | **0.9790** | **0.9971** |
| *30%* | 0.9682 | 0.9464 | 0.9801 | 0.9701 | 0.9508 | 0.7597 | 0.9704 | 0.9533 | 0.9495 | 0.9659 | 0.9480 | 0.9820 | **0.9819** | **0.9753** | **0.9931** |
| *40%* | 0.9404 | 0.9031 | 0.9422 | 0.9420 | 0.9080 | 0.7420 | 0.9441 | 0.9128 | 0.9013 | 0.9383 | 0.9079 | 0.9501 | **0.9528-0.9548** | **0.9301-0.9345** | **0.9577-0.9627** |
| *50%* | 0.9376 | 0.8950 | 0.9300 | 0.9397 | 0.9011 | 0.6110 | 0.9424 | 0.9085 | 0.8777 | 0.9359 | 0.9023 | 0.9412 | **0.9508-0.9524** | **0.9231-0.9282** | **0.9501-0.9541** |
| *60%* | 0.9339 | 0.8865 | 0.9187 | 0.9366 | 0.8951 | 0.4811 | 0.9396 | 0.9021 | 0.8477 | 0.9330 | 0.8960 | 0.9237 | **0.9478-0.9499** | **0.9165-0.9219** | **0.9402-0.9439** |
| *70%* | 0.9303 | 0.8799 | 0.8894 | 0.9323 | 0.8852 | 0.3257 | 0.9355 | 0.8927 | 0.6381 | 0.9301 | 0.8881 | 0.9097 | **0.9432-0.9459** | **0.9083-0.9138** | **0.9281-0.9323** |
| *80%* | 0.9018 | 0.8340 | 0.8327 | 0.8948 | 0.8295 | 0.2011 | 0.9063 | 0.8479 | 0.5914 | 0.9024 | 0.8430 | 0.8621 | **0.9106-0.9160** | **0.8571-0.8663** | **0.8771-0.8851** |
| *90%* | 0.8677 | 0.7859 | 0.7991 | 0.8547 | 0.7726 | 0.0859 | 0.8709 | 0.7956 | 0.3539 | 0.8686 | 0.7895 | 0.8315 | **0.8725-0.8800** | **0.8011-0.8122** | **0.8401-0.8506** |

Table 2. Correlation (β) comparison on Lena, Camera man and MRI images

| | *IBDNDF [9]* | | | *DBUTMWMF [11]* | | | *UWMF [12]* | | | *Lu`s three-values-weighted [13]* | | | ***AMFWMF*** | | |
|---|---|---|---|---|---|---|---|---|---|---|---|---|---|---|---|
| | *Lena* | *Camera man* | *MRI image* | *Lena* | *Camera man* | *MRI image* | *Lena* | *Camera man* | *MRI image* | *Lena* | *Camera man* | *MRI image* | ***Lena*** | ***Camera man*** | *MRI image* |
| *10%* | 0.9542 | 0.9174 | 0.9807 | 0.9574 | 0.9227 | 0.4825 | 0.9580 | 0.9251 | 0.9818 | 0.9377 | 0.9003 | 0.9811 | **0.9744** | **0.9576** | **0.9877** |
| *20%* | 0.9384 | 0.8947 | 0.9681 | 0.9468 | 0.9052 | 0.4128 | 0.9489 | 0.9128 | 0.9606 | 0.8944 | 0.8529 | 0.9713 | **0.9635** | **0.9426** | **0.9813** |
| *30%* | 0.9199 | 0.8671 | 0.9535 | 0.9354 | 0.8885 | 0.3982 | 0.9361 | 0.8955 | 0.8994 | 0.8565 | 0.7923 | 0.9621 | **0.9496** | **0.9225** | **0.9724** |
| *40%* | 0.8902 | 0.8227 | 0.9098 | 0.9016 | 0.8438 | 0.3865 | 0.9043 | 0.8497 | 0.8646 | 0.8168 | 0.7423 | 0.9227 | **0.9048-0.9156** | **0.8508-0.8630** | **0.9353-0.9424** |
| *50%* | 0.8662 | 0.7886 | 0.8871 | 0.8825 | 0.8141 | 0.3702 | 0.8848 | 0.8204 | 0.8186 | 0.7894 | 0.7127 | 0.9017 | **0.8861-0.8962** | **0.8221-0.8370** | **0.9181-0.9264** |
| *60%* | 0.8369 | 0.7553 | 0.8525 | 0.8599 | 0.7851 | 0.3544 | 0.8633 | 0.7929 | 0.7693 | 0.7625 | 0.6813 | 0.8702 | **0.8641-0.8744** | **0.7940-0.8080** | **0.8916-0.9001** |
| *70%* | 0.8099 | 0.7245 | 0.8195 | 0.8312 | 0.7454 | 0.3317 | 0.8331 | 0.7588 | 0.5689 | 0.7437 | 0.6537 | 0.8441 | **0.8343-0.8456** | **0.7604-0.7736** | **0.8627-0.8712** |
| *80%* | 0.7693 | 0.6699 | 0.7715 | 0.7614 | 0.6508 | 0.2757 | 0.7791 | 0.6921 | 0.5775 | 0.7244 | 0.6191 | 0.8031 | **0.7772-0.7995** | **0.6901-0.7129** | **0.8107-0.8261** |
| *90%* | 0.6976 | 0.6074 | 0.7016 | 0.6817 | 0.5640 | 0.2161 | 0.7039 | 0.6136 | 0.4424 | 0.6806 | 0.5676 | 0.7543 | **0.7032-0.7253** | **0.6116-0.6315** | **0.7656-0.7873** |

Table 3. Structural similarity index (SSIM) comparison on Lena, Camera man and MRI images

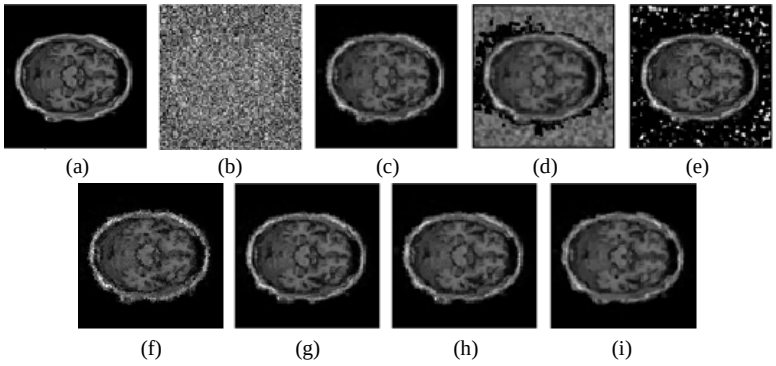


Figure 4. Denoising results for 80% impulse noise on MRI, a) Original image b) Noisy image c) IBDNDF [9] d) DBUTMWMF [11] e) UWMF [12] f) Lu`s three-values-weighted [13] g) AMFWMF (initial window size=3) h) AMFWMF (initial adaptive median window size=5 i) AMFWMF (initial adaptive median window size=7)

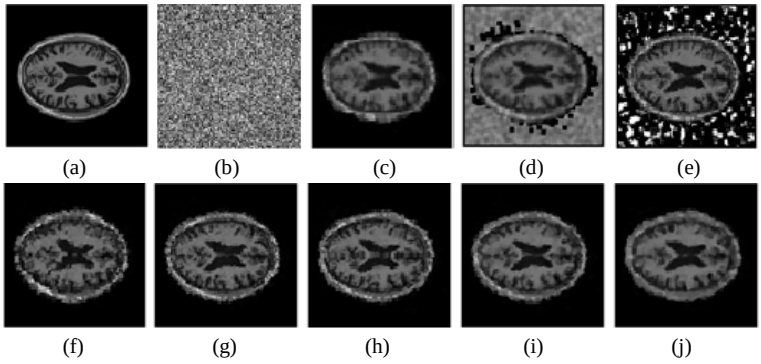


Figure 5. Denoising results for 90% impulse noise on MRI, a) Original image b) Noisy image c) IBDNDF [9] d) DBUTMWMF [11] e) UWMF [12] f) Lu`s three-values-weighted [13] g) AMFWMF (initial window size=3) h) AMFWMF (initial adaptive median window size=5 i) AMFWMF (initial adaptive median window size=7 j) AMFWMF (initial adaptive median window size=9)

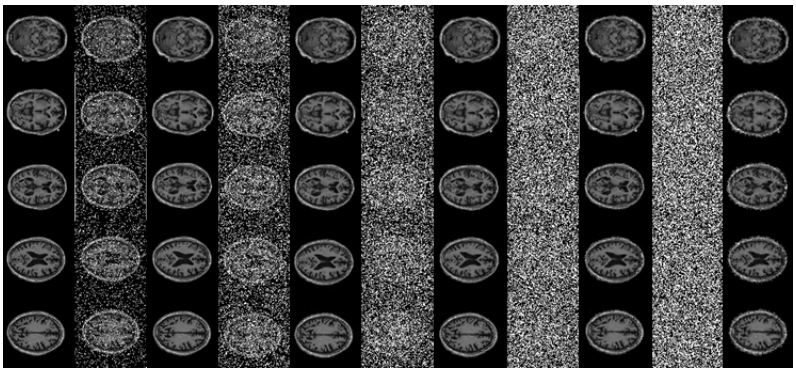

Figure 6. Results of applying the proposed filter on MRI images corrupted by different levels of impulse noise. The 1th column is original MRI images, even columns (2nd through 10th) are respectively the original MRI with 20%, 40%, 60%, 80% and 90% impulse noise, odd columns (3rd through 11th) show the denoising results of their previous columns.

to yield better structural metrics than any other denoising filters in the presence of different impulse noise intensities. Denoising with this method is shown to preserve image details and edges. These qualities are very important when dealing with corrupted MRI images. The high structural metric measures prove the similarity between the denoised image and the original noise-free image. This filtering method also allows edge detection algorithms to become immune and resilient to noise, enhancing image segmentation, object recognition, feature extraction, pattern classification, and deriving structural and functional measurements in medical imaging specially MRI images.

## ACKNOWLEDGEMENTS

We are grateful for the continued support from the National Science Foundation (NSF) under NSF grants CNS-1532061, CNS-0959985, CNS-1551221, HRD-0833093, and IIP 1338922. We also greatly appreciate the support of the Ware Foundation. This material is based upon work supported by the National Science Foundation Graduate Research Fellowship under Grant No. (DGE-1610348). Any opinion, findings, and conclusions or recommendations expressed in this material are those of the author(s) and do not necessarily reflect the views of the National Science Foundation.

## REFERENCES

[1] K. M. Moon and M. D. Patil, B. Parmar, "Image Restoration Using Adaptive Switching Median Filter," *in Proceedings of the IEEE Conference on Computational Intelligence and Computing Research*, 2010, pp. 1-4.

[2] L. Lin, X. Meng, X. Liang, "Reduction of Impulse Noise in MRI Images Using Block-based Adaptive Median Filter," *in Proceedings of the IEEE Conference on Medical Imaging Physics and Engineering*, 2013, pp. 132-134.

[3] S. Vishaga and S. L. Das, "A Survey on Switching Median Filters for Impulse Noise Removal," *in Proceedings of the IEEE Conference on Circuit, Power and Computing Technologies*, 2015, pp.1-6.

[4] R. C. Gonzalez and R. E. Woods, *Digital image processing*, 3th ed., Upper Saddle River, New Jersy,USA, Prentice-Hall: 2006.

[5] S. J. Ko and Y. H. Lee, "Center Weighted Median Filter," *IEEE Trans. Circuits Systs.*, vol. 38, no.9, pp 984-993, 1991.

[6] Y. Dong and S. Xu, "A New Directional Weighted Median Filter for Removal of Random-Valued Impulse Noise," IEEE Signal Process. Lett., vol. 14, no. 3, pp. 193- 196, 2007.

[7] V. V. Khryaschev, A. L. Priorov, I. V. Apalkov, P. S. Zvonarev, "Impulse Denoising Using Adaptive Switching Median Filter," *in Proceedings of the IEEE Conference on Circuit, Power and Computing Technologies*, 2005, pp.117-120.

[8] S. Esakkirajan, T. Veerakumar, A. N. Subramanyam, C.H. PremChand, "Removal of High Dendity Salt and Pepper noise Trhough Modified Decision based Unsymmetrical Trimmed Median Filter," IEEE Signal Process. Lett., vol.18, no.5, pp. 287-290, 2011.

[9] I. F. Jafar, R. A. AlNa'mneh, K.A. Darabkh, "Efficient Improvements on the BDND Filtering Algorithm for the Removal of High-Density Impulse Noise," IEEE Trans. Image Process., vol. 22, no. 3, pp. 1223-1232, 2013.

[10] P. E. Ng and K. K. Ma, "A Switching Median Filter With Boundary Discriminative Noise Detection for Extremely Corrupted Images," IEEE Trans. Image Process., vol. 15, no. 6, pp.1506-1516, 2006.

[11] K. Vasanth, T. G. Manjunath, N. Raj "A Decision Based Unsymmetrical Trimmed Modified Winsorized Mean Filter for the Removal of High Density Salt and Pepper Noise in Images and Videos," Procedia Comput. Sci., no. 54, pp. 595-604, 2015.

[12] C. Kandemir, C. Kalyoncu, Ö. Toygar, "A weighted mean filter with spatial-bias elimination for impulse noise removal," Digital Signal Process., vol. 46, pp. 164–174, 2015.

[13] C. T. Lu, Y. Y. Chen, L. L. Wang, , C. F. Chang, "Removal of salt-and-pepper noise in corrupted image using three-values-weighted approach with variable-size window," Pattern Recognition Letters, vol. 80, pp. 188–199, 2016.

[14] H. Hwang and R. A. Haddad, "Adaptive Median Filters: New Algorithms and Results," IEEE Trans. Image Process., vol.4, no. 4, pp. 499-502, 1995.

[15] Z. Zhou, "Cognition and Removal of Impulse Noise With Uncertainty," IEEE Trans. Image Process., vol. 21, no. 7, 2012.

[16] C. Kalyoncu1, Ö. Toygar, H. Demirel, "Interpolation-based impulse noise removal," IET Image Process., vol.7, no. 8, pp. 777-785, 2013.

[17] Z. Wang, A. C. Bovik, H. R. Sheikh, E. P. Simoncelli, "Image Quality Assessment: From Error Visibility to Structural Similarity," IEEE Trans. Image Process., vol. 13, no. 4, pp. 600-612, 2004.